Electronic Supplementary Material (ESI) for Inorganic Chemistry Frontiers.

Supporting Information

Ultrasmall MoP embraced in nitrogen-doped carbon hybrid frameworks for highly efficient hydrogen evolution reaction in both acid and alkaline solutions

Xiaokang Huang, Xiang Wang, Pengbo Jiang, Kai Lan, Jiaheng Qin, Li Gong, Kaizhi Wang, Ming Yang, Lei Ma and Rong Li*

State Key Laboratory of Applied Organic Chemistry (SKLAOC), The Key Laboratory of Catalytic Engineering of Gansu Province, College of Chemistry and Chemical Engineering, Lanzhou University, Lanzhou, 730000, PR China.

*Corresponding Author.

E-mail: liyirong@lzu.edu.cn; Fax: +86- 931-891-2582; Tel: +86-18919803060.

Materials

Ammonium molybdate tetrahydrate ($(NH_4)_6Mo_7O_{24}\cdot 4H_2O$), urea, citric acid (CA), aceton, sodium hydroxide (NaOH), diammonium hydrogen phosphate ($(NH_4)_2HPO_4$), hydrochloric acid (HCl), and N,N-Dimethylformamide (DMF) were acquired from Shanghai Macklin Biochemical Co. Ltd.. The commercial Pt/C catalyst (20 wt% platinum on carbon black) was purchased from Aladdin Industrial Inc (Shanghai, China). High purity water(18.2 MΩ·cm) was supplied by a water purification system throughout the experimental process. Nafion solution (0.5 wt%) were acquired from

Alfa Aesar . All reagents were of analytical grade and used as received in the entire experiment.

Table S1. The preparation conditions of the carbon substrates. The carbon precursor was prepared from the mixture of acetone and NaOH via a facile stationary method. All the calcining processes were conducted in the tube furnace with heating rate of 5 ℃/min under N_2 gas flow.

Sample	**Raw materials**	**Calcining processes**	
		first step	**second step**
NCF-8	0.02 g carbon precursor, 3 g urea	600 ℃, 60 min	800 ℃, 80 min
NCF		600 ℃, 60 min	900 ℃, 80 min
NCF-10		600 ℃, 60 min	1000 ℃, 80 min

Table S2. The preparation conditions of as-synthesized samples. All MoP-based samples were prepared from mixture of raw materials containing 0.02 g carbon substrate through the calcining process at 750 ℃ for 6 h with heating rate of 2.5 ℃/min under H_2/Ar mixed gas (with 10% H_2) flow.

Sample	**Raw materials**			
	carbon substrate	**$(NH_4)_6Mo_7O_{24}$**	**$(NH_4)_2HPO_4$**	**critic acid**
MoP@NCF	NCF	0.2 mmol	1.4 mmol	2.8 mmol
MoP@NCF -CA0	NCF	0.2 mmol	1.4 mmol	0
MoP@NCF -8	NCF-8	0.2 mmol	1.4 mmol	2.8 mmol
MoP@NCF -10	NCF-10	0.2 mmol	1.4 mmol	2.8 mmol
MoP@Urea	urea	0.2 mmol	1.4 mmol	2.8 mmol

Table S3. The C, N contents of as-synthesized MoP-based electrocatalysts. All samples were measured by elemental analyzer (EA).

	Sample	MoP@ NCF	MoP@ NCF-10	MoP@ NCF-8	MoP@NCF- CA0	MoP@ urea
C	Mass Fraction (%)	14.20	17.16	16.45	4.01	12.26
	Atomic Fraction (%)	1.18	1.43	1.37	0.33	1.02
N	Mass Fraction (%)	0.66	0.60	0.77	0.35	0.51
	Atomic Fraction (%)	0.047	0.043	0.055	0.025	0.036

Electrode preparation and electrochemical measurements

The working electrode was prepared as follows: 4 mg as prepared catalyst powder was suspended in 1 mL DMF-high purity water mixed solution (volume ratio of DMF : water = 3 : 1) contained 30 μL Nafion solution (0.5 wt%) to obtain a homogeneous ink by sonication. After that, 5μL of fresh ink was spread onto a glass carbon electrode with a diameter of 3 mm (catalyst loading of 0.285 mg cm^{-2}). Electrochemical measurement was performed using a computer-controlled electrochemical workstation (CHI660E, CH Instrument, Shanghai Chenhua Equipment, China) with an Ag/AgCl (with salt bridge in 3.0 M KCl solution) electrode and a graphite rod in 0.5 M H_2SO_4 or 1.0 M KOH electrolyte solutions. The two electrodes used as the reference electrode and counter electrode, respectively. All measured potentials (vs. Ag/AgCl) were converted to a reversible hydrogen electrode (RHE) using the Nernst equation: $E_{RHE} = E_{Ag/AgCl} + E^{\theta}_{Ag/AgCl} + 0.059\,pH\,(E^{\theta}_{Ag/AgCl} = 0.209\ V)$. All the electrochemical measurements were not iR compensated and conducted at room temperature.

Characterization

The scanning electron microscopy (SEM) images were observed on a Hitachi S4800 (Chiyoda-ku, Tokyo, Japan) operated under high vacuum with an accelerating voltage of 7 kV. Transmission electron microscopy (TEM) images and high resolution transmission electron microscopy (HR-TEM) images were recorded on a FEI (Talos F200S G2, USA) microscope with capabilities for energy-dispersive X-ray spectroscopy (EDX, Super-X EDS Detector, USA) operating at 200 KV. The crystal structure data were acquired on a Rigaku D/max-2400 diffractometer, using Cu-Kα radiation as X-ray source in the range of 10-90°. Raman spectra were obtained on Jobin-Y von LabRam HR80 spectrometer (Horiba Jobin-Y von, Inc.) with 532 nm laser excited. The surface area and pore sizes were measured using Electronic Supplementary Material (ESI) for the Brunauer–Emmett–Teller (BET) and Barrett–Joyner–Halenda (BJH) methods by utilizing a Tristar II 3020 instrument. XPS measurements were performed on a PHI-5702 instrument equipped with an Mg-Kα source (1253.6 eV) at room temperature under 3×10^{-8} Torr. For elemental content estimation, inductively coupled plasma (ICP) and elemental analyzer (EA) were used.

HER measurements

The HER activities of all samples were measured on the same electrochemical workstation and investigated by Linear sweep voltammetry (LSV) within the range of -0.6 to 0.2 V vs. RHE at a slow scan rate of 5 mV s^{-1}. 1.0 M KOH and 0.5 M H_2SO_4 (purged with pure N_2) was used as the electrolyte. The Tafel slope was calculated according to the Tafel equation. The stability was tested by means of chronoamperometry measurements. It was also evaluated by cycling the electrode potential (-0.6 V to 0.2 V) for 2000 cycles at 0.2 V s^{-1}, after which the LSV were recorded. Electrochemical impedance spectroscopy (EIS) was performed in 1.0 M KOH and 0.5 M H_2SO_4 in the frequency range 10^5–0.01 Hz with ac amplitude of 10 mV. All the EIS data was normalized to the geometric surface area of the working electrode.

Turnover frequency (TOF) calculation

Turnover frequency (TOF) calculation of the catalysts: The TOF value is calculated from the equation.[1, 2]

$$TOF= (j\times A)/(4\times F\times m) \tag{1}$$

j is the current density at overpotential of 150 mV. A is the area of the glass carbon electrode. F is the faraday constant (a value of 96485.3 C/mol). m is the number of moles of the active materials that are deposited onto with the area of 0.07 cm^{-2}. All the Mo atoms were assumed to be accessible for catalysis the HER. The mass fraction of Mo atoms in as-synthesized MoP-based electrocatalysts is 53.77% measured by inductively coupled plasma (ICP).

Table S4. The turnover frequency (TOF) calculation of MoP@NCF and the contrast samples in acid and alkaline electrolytes at the overpotential of 150 mV.

Samples	MoP@NCF	MoP@ NCF -10	MoP@ NCF -8	MoP@NCF -CA0	MoP@Urea
$\lvert j\rvert$ in acid (mA cm^{-2})	24.88	5.02	0.23	0.91	4.66
TOF in acid (s^{-1})	0.0817	0.0165	0.0008	0.0030	0.0153
$\lvert j\rvert$ in alkaline (mA cm^{-2})	18.80	8.07	0.77	0.82	3.22
TOF in alkaline (s^{-1})	0.0617	0.0265	0.0025	0.0027	0.0106

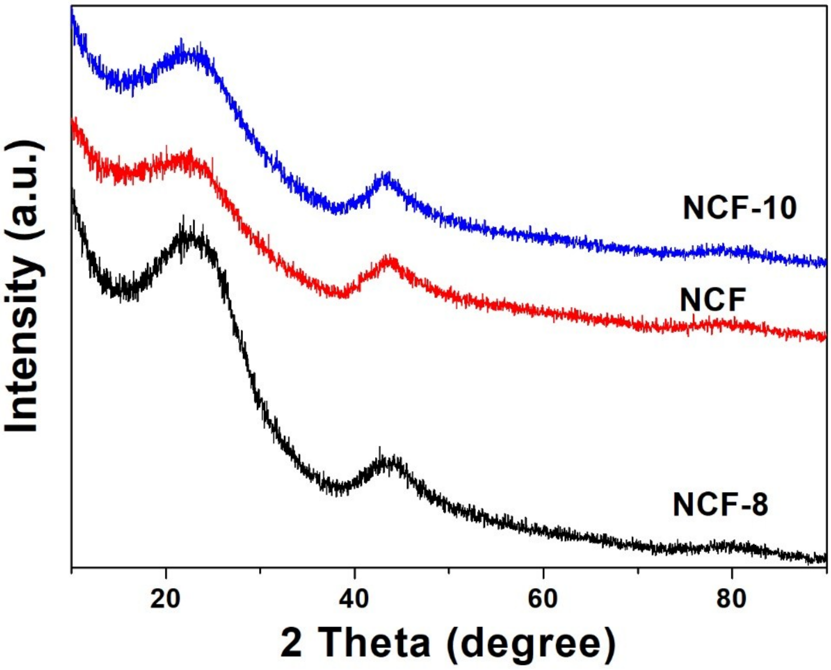

Figure S1. XRD patterns of NCF, NCF-10 and NCF-8.

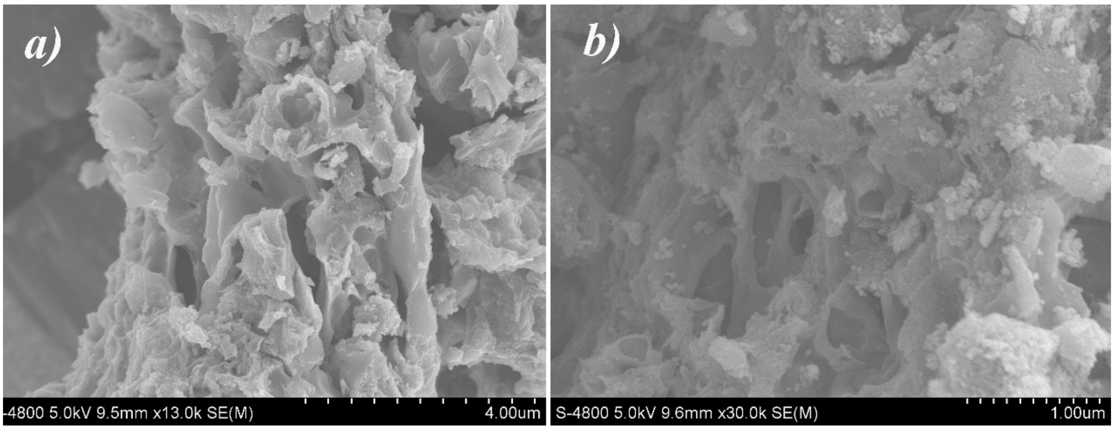

Figure S2. SEM images of MoP@NCF under different magnifications.

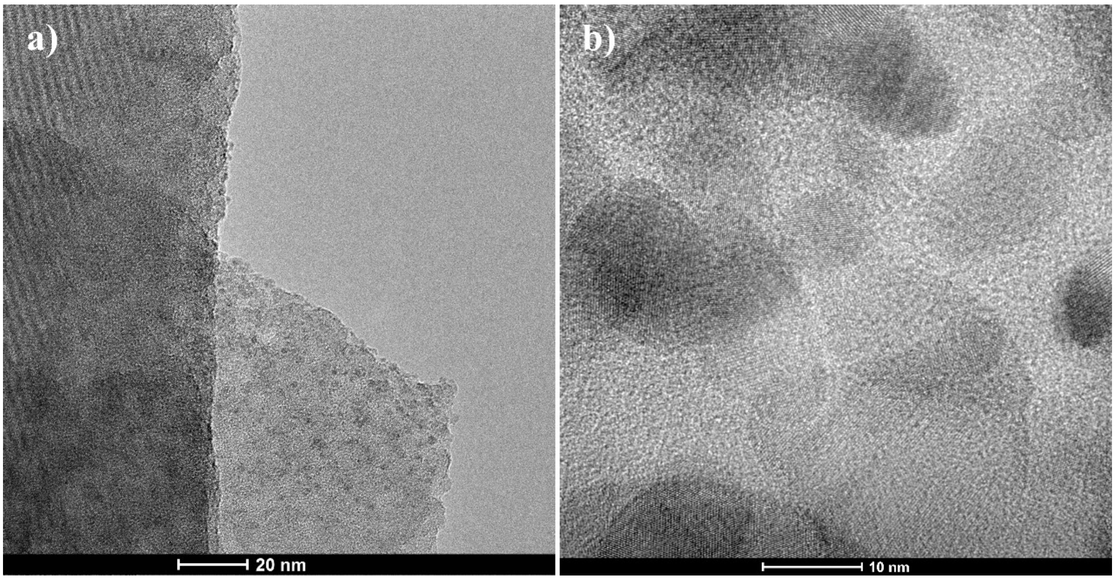

Figure S3. (a) The TEM image and (b) HR-TEM image of MoP@NCF.

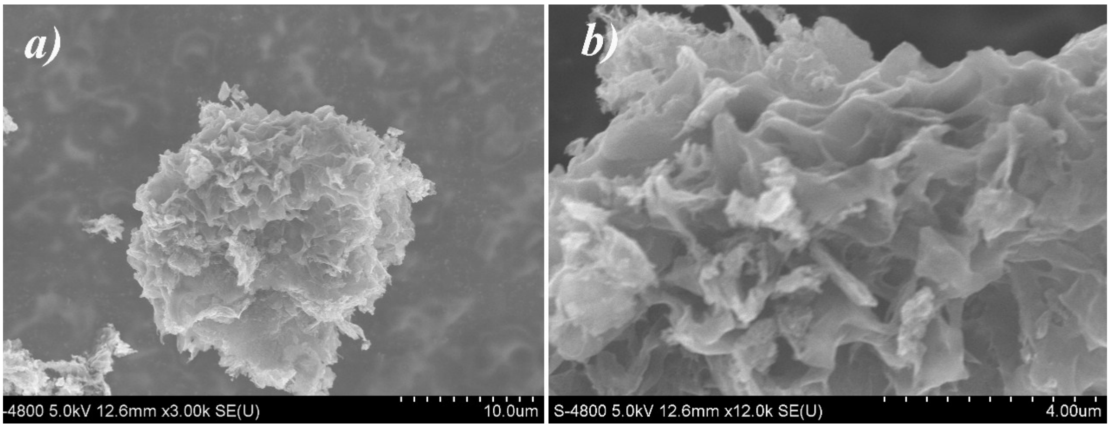

Figure S4. SEM images of NCF under different magnifications.

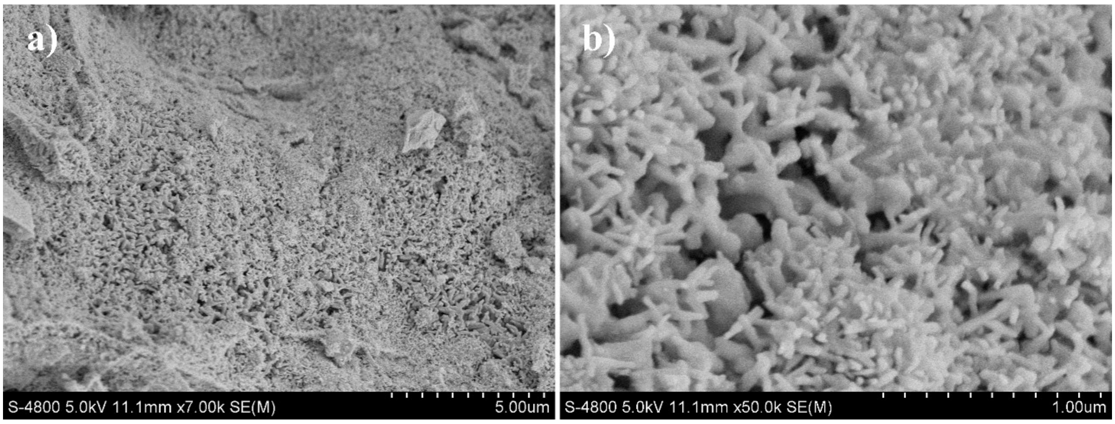

Figure S5. SEM images of MoP@NCF-CA0 under different magnifications.

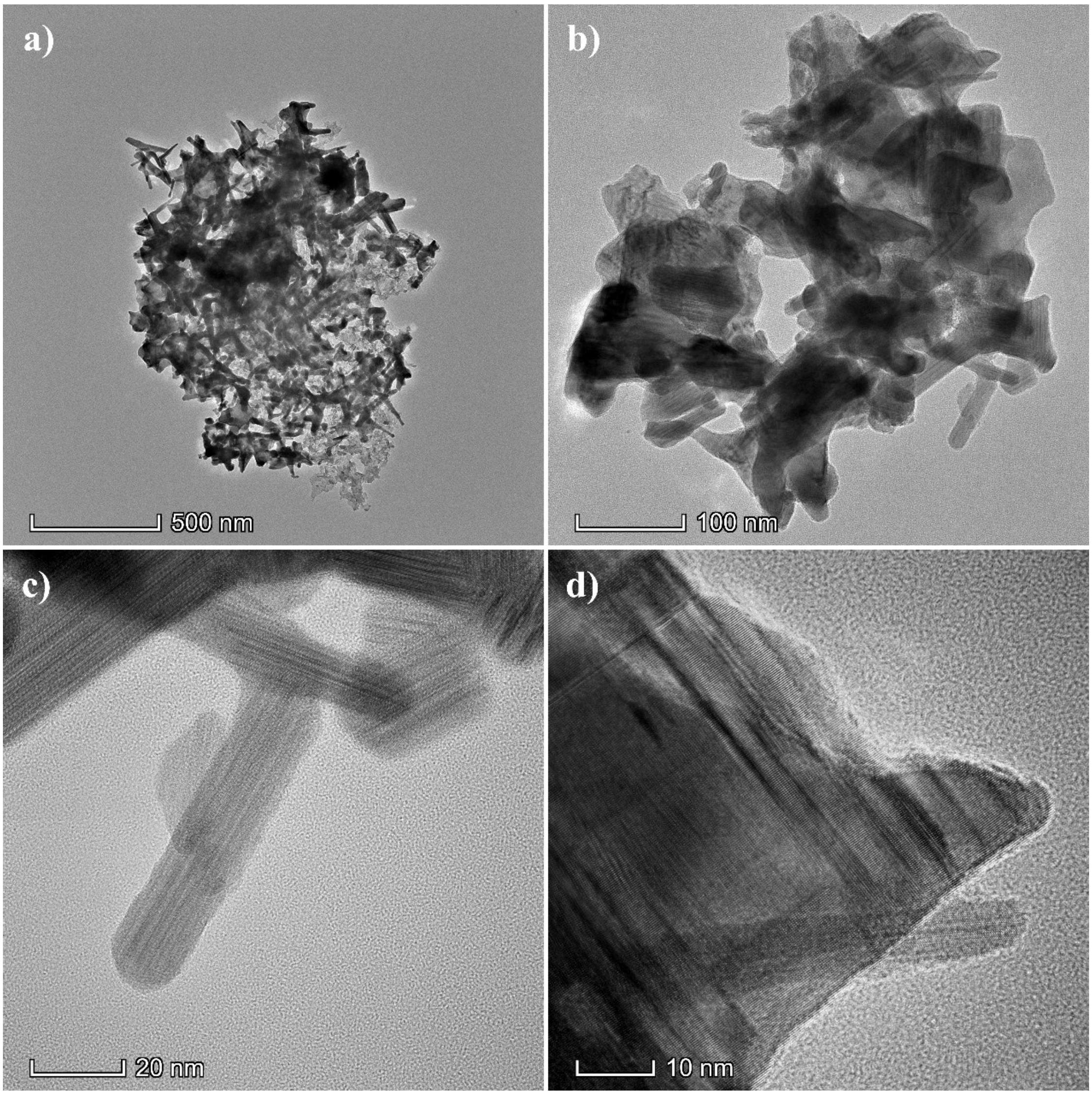

Figure S6. (a) (b) The TEM images and (c) (d) HR-TEM images of MoP@NCF-CA0 under different magnifications.

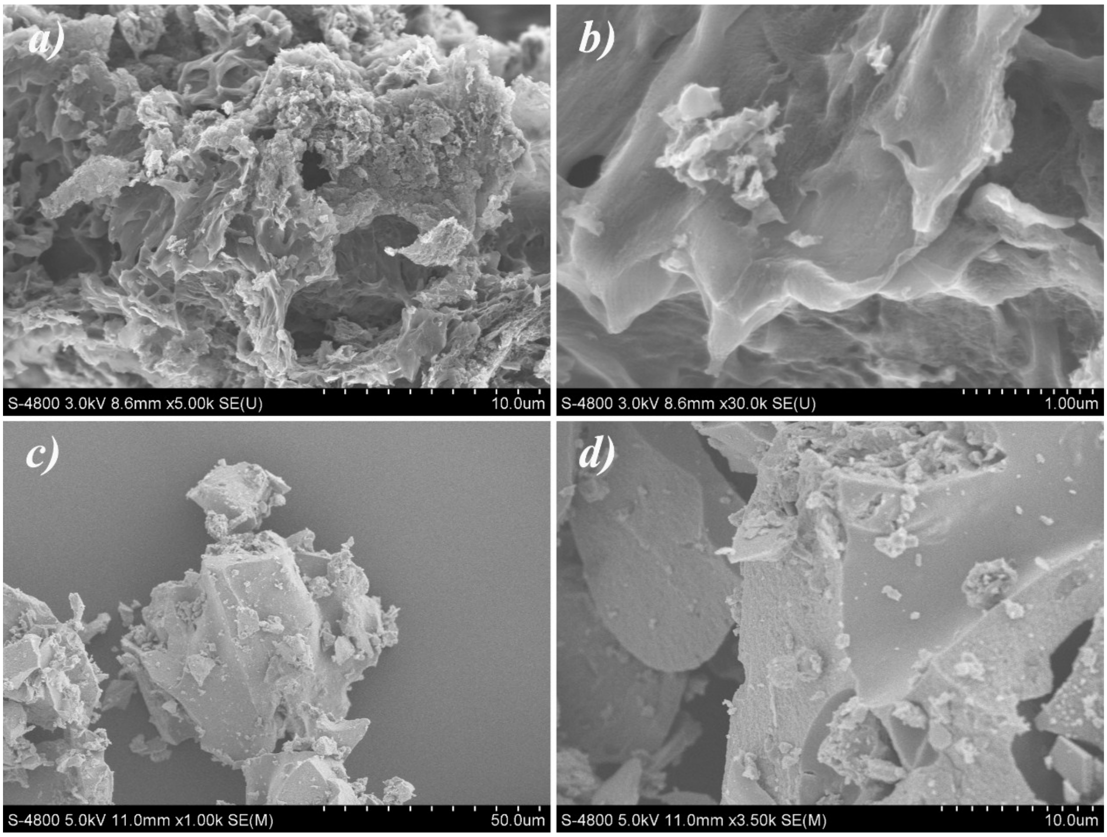

Figure S7. SEM images of (a) (b)| NCF-8, (c) (d) MoP@NCF-8 under different magnifications.

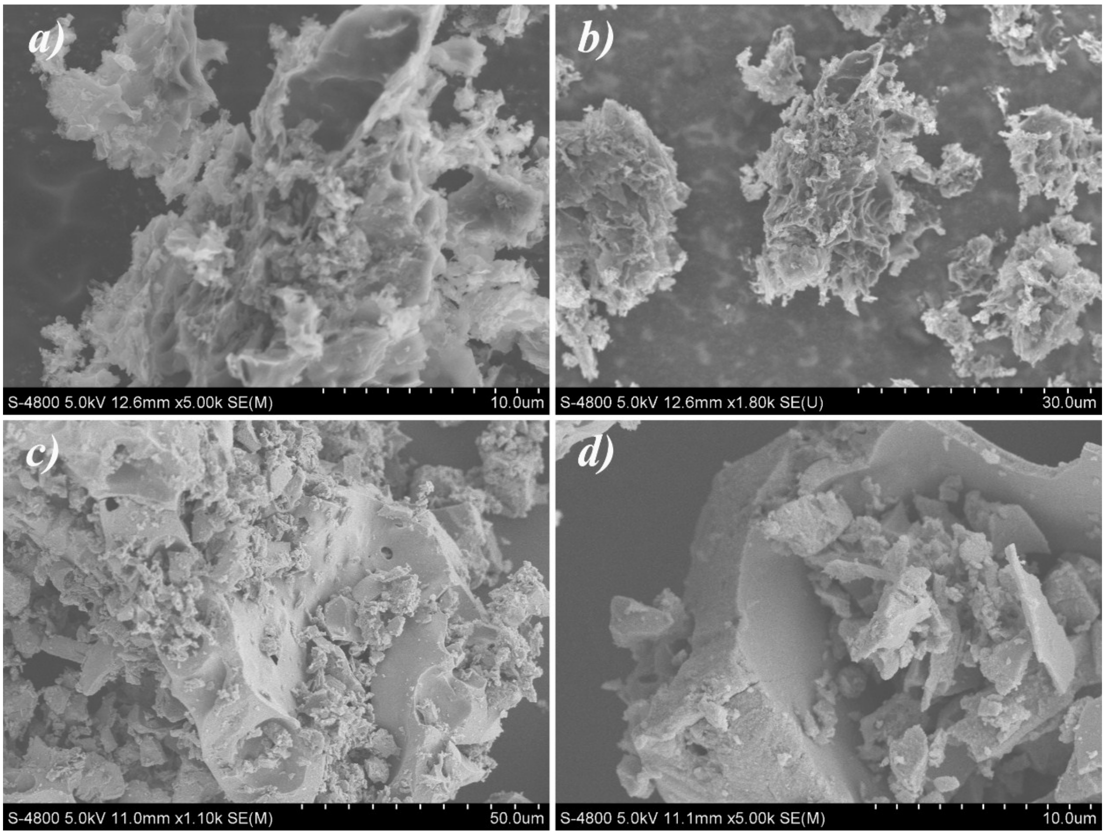

Figure S8. SEM images of (a) (b)| NCF-10, (c) (d) MoP@NCF-10 under different magnifications.

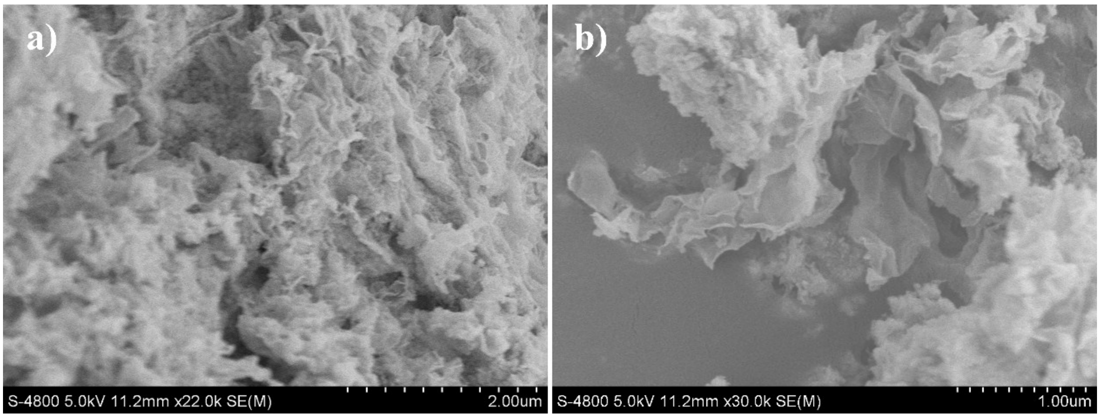

Figure S9. SEM images of MoP@Urea under different magnifications.

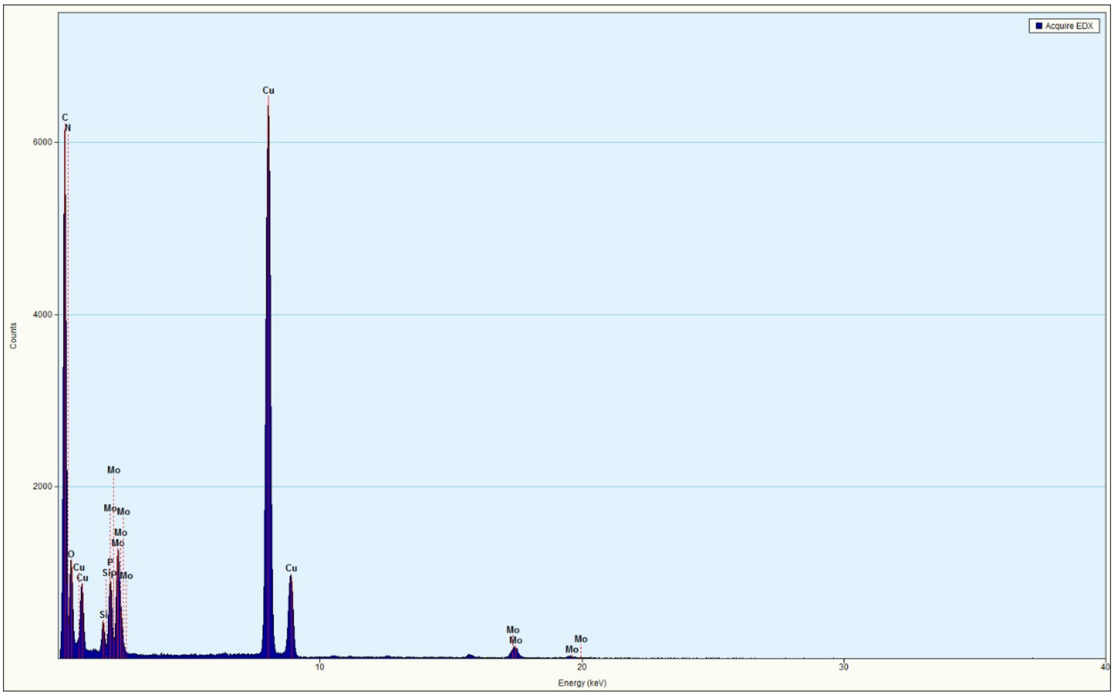

Figure S10. EDS spectrum of the MoP@NCF.

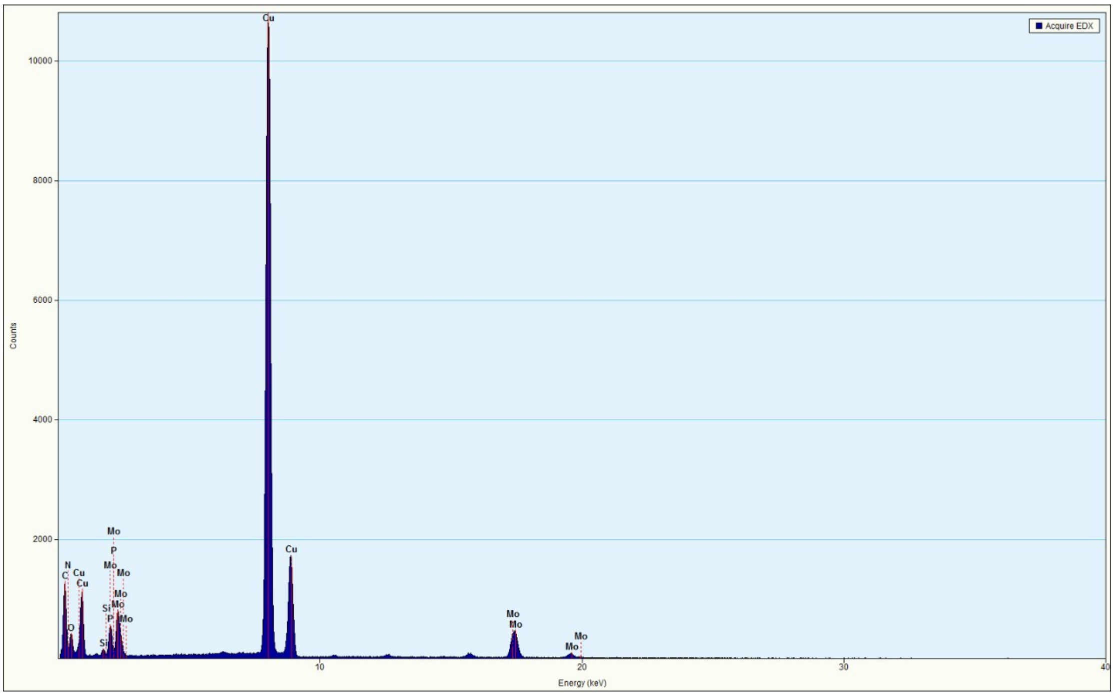

Figure S11. EDS spectrum of the MoP@NCF-CA0.

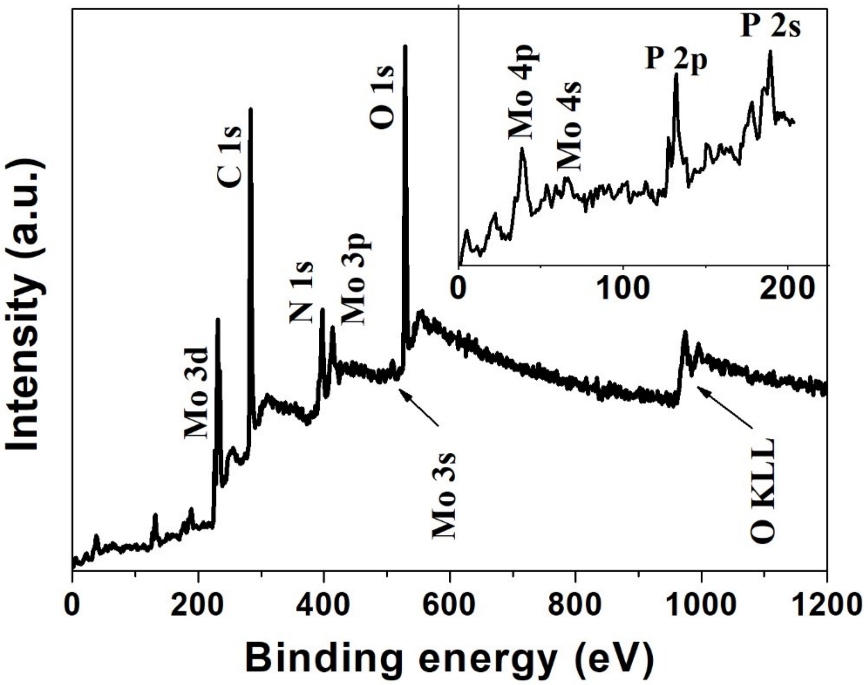

Figure S12. Full-scan XPS spectra of MoP@NCF.

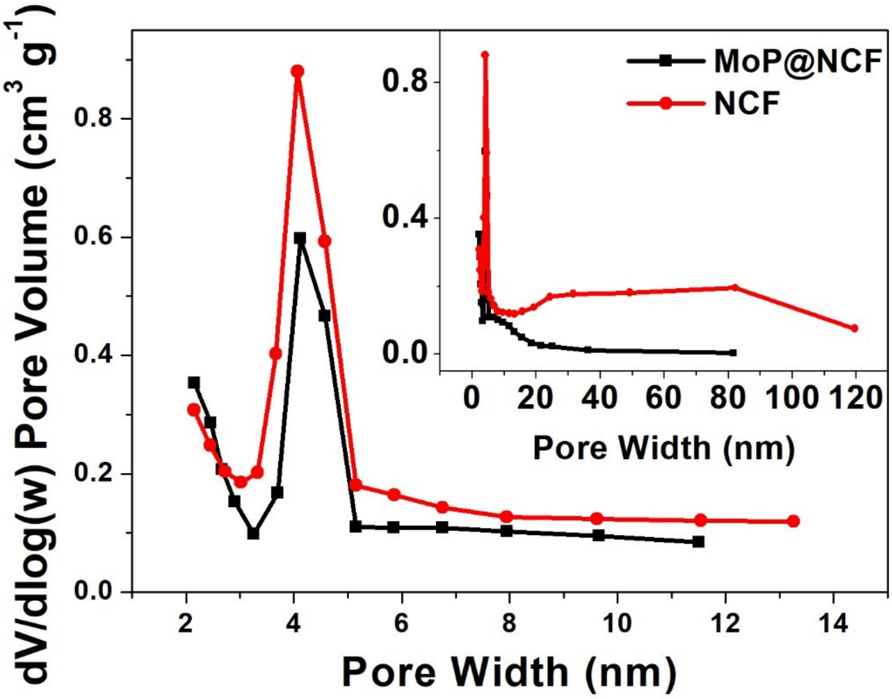

Figure S13. The pore size distribution of MoP@NCF in comparison to NCF.

Table S5. BET surface area of MoP@NCF and the contrast samples.

Sample name	**BET Surface Area (m^2 g^{-1})**	**t-Plot Micropore Area (m^2 g^{-1})**	**t-Plot External Surface Area (m^2 g^{-1})**
MoP@NCF	247.43	77.38	170.05
MoP@NCF -10	20.53	7.24	13.29
MoP@NCF -8	54.77	20.22	34.55
MoP@NCF-CA0	5.7	1.42	4.28
MoP@Urea	29.48	11.24	18.24
NCF	810.93	406.28	404.64
NCF-10	801.68	357.7	443.98
NCF-8	1122.59	592.68	529.91

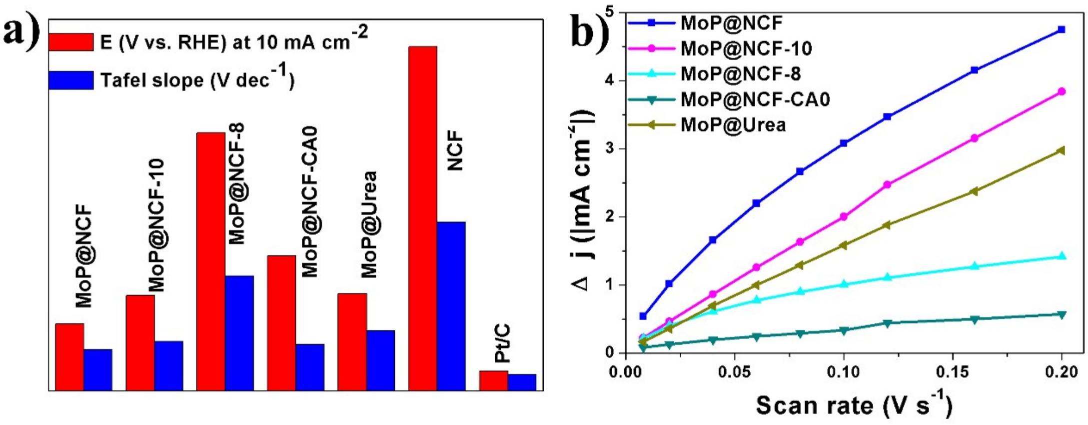

Figure S14. Comparison of electrocatalysis performance of MoP@NCF and the contrast samples in 0.5 M H_2SO_4 : (a) the overpotentials at 10 mA cm^{-2} and the corresponding Tafel slopes, (b) the double layer capacity C_{dl}.

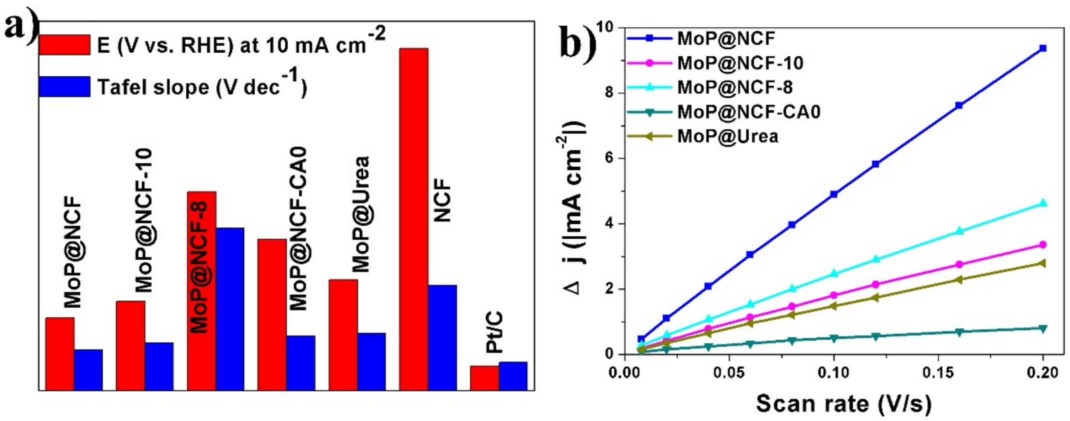

Figure S15. Comparison of electrocatalysis performance of MoP@NCF and the contrast samples in 1 M KOH : (a) the overpotentials at 10 mA cm^{-2} and the corresponding Tafel slopes, (b) the double layer capacity C_{dl}.

Table S6. Comparison of the overpotential at the current density of 10 mA cm^{-2} and Tafel slopes of MoP@NCF and contrast samples.

Sample		MoP @NCF	MoP@ NCF-10	MoP@ NCF-8	MoP@ NCF-CA0	MoP @urea	NCF	Pt/C
acid electrolyte	overpotential/mV	121.8	173.9	470	246	177	627	36
	Tafel/mV dec^{-1}	75.2	89.8	209.3	84.5	109.7	307.5	29.7
alkaline electrolyte	overpotential/mV	129.5	159	354	270	197	610	43.7
	Tafel/mV dec^{-1}	72.4	84.9	289.4	96.9	101.8	187.4	50.2

Double-layer capacitances (Cdl) calculation

To illustrate the influence of the electrochemical active surface areas (ECSA) of as-synthesized electrocatalysts samples, the double-layer capacitances (Cdl) has been carried out using a simple cyclic voltammetry (CV) method with the voltage scan rates from 8 to 200 mV s^{-1} at the potential around the open circuit potential (OCP) without any redox reactions. The double layer capacitance of as-synthesized electrocatalysts was estimated by plotting the $\Delta J = |J_a - J_c|$ (J_a and J_c are the current density of different current direction under a series of scan rates) at 0.05 V vs RHE against the scan rate in both acid and alkaline electrolytes. The linear slope is equivalent to twice of the double-layer capacitance Cdl, which can be used to represent the electrochemical active surface area. The Cdl values can be calculated from the equation.

$$\Delta J = |J_a - J_c| = kv + b \tag{2}$$

$$Cdl = k/2 \tag{3}$$

k is the linear slope of plots image of ΔJ versus scan rate , and b is constant.

Table S7. the double-layer capacitances (Cdl) of MoP@NCF and contrast samples.

Sample	MoP@NCF	MoP@ NCF-10	MoP@ NCF-8	MoP@NCF -CA0	MoP@urea
Acid electrolyte/s^{-1}	10.80	9.50	2.99	1.30	7.24
Alkaline electrolyte/s^{-1}	23.14	8.26	11.29	1.87	6.85

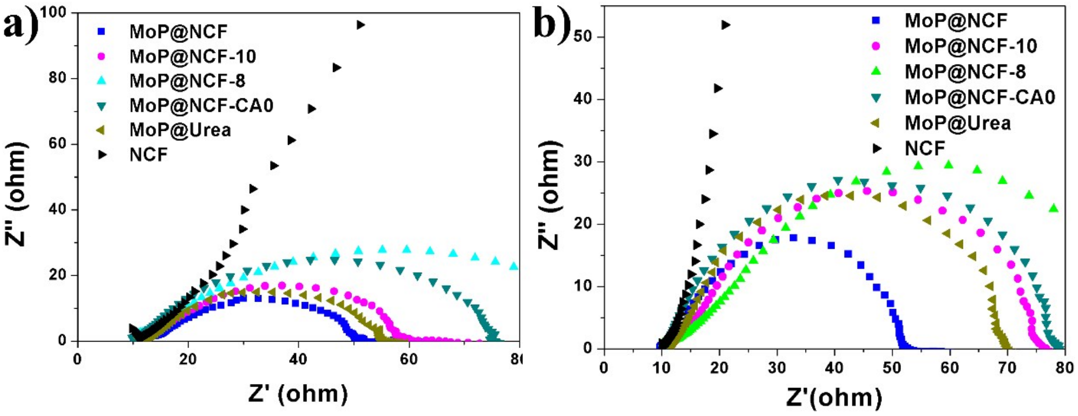

Figure S16. Nyquist plots of MoP@NCF and the contrast samples (a) at -130 mV in acidic solution and (b) at -140 mV in alkaline solution

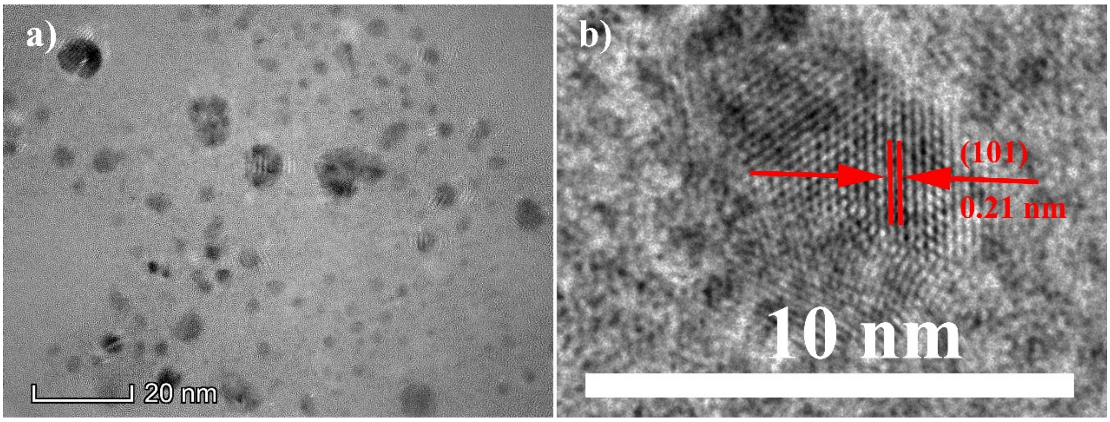

Figure S17. The TEM (a) and HR-TEM (b) images of MoP@NCF after long-term durability test in acid electrolyte.

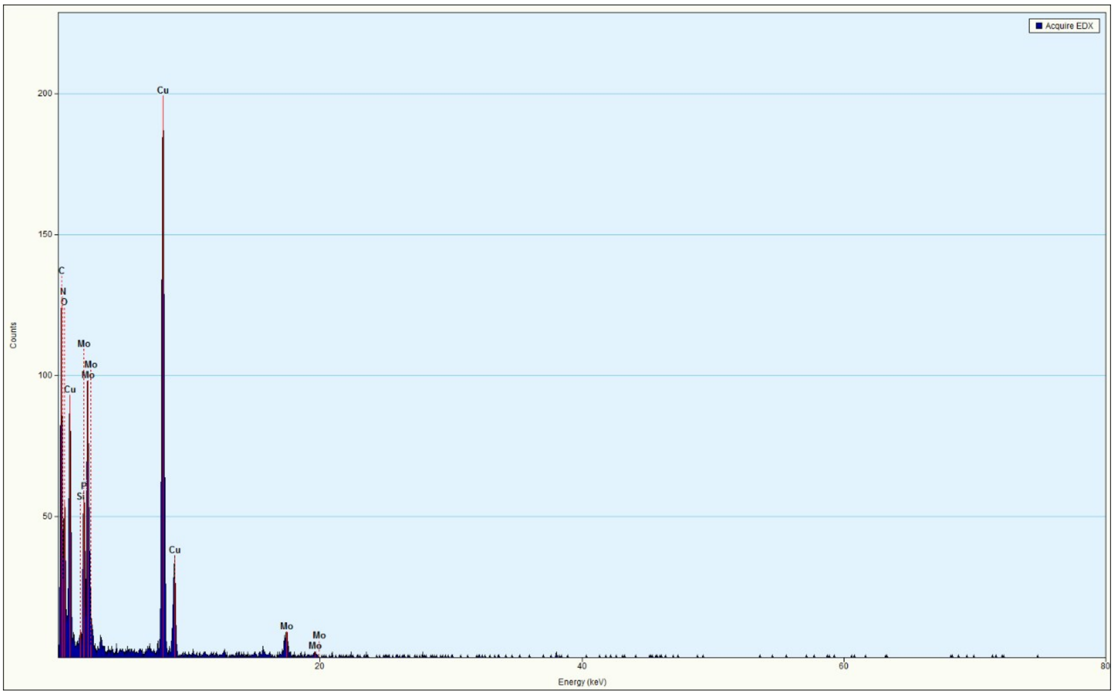

Figure S18. The EDS spectrum of MoP@NCF after long-term durability test in acid electrolyte.

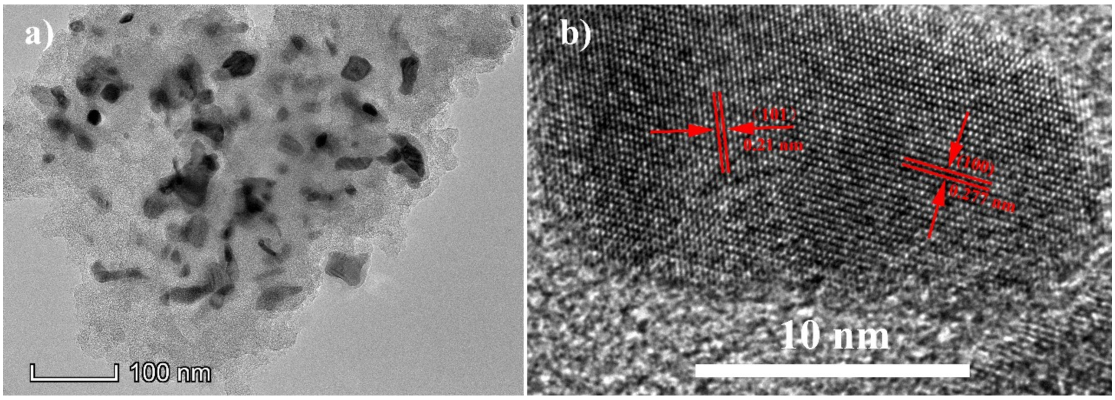

Figure S19. The TEM (a) and HR-TEM (b) images of MoP@NCF after long-term durability test in alkaline electrolyte.

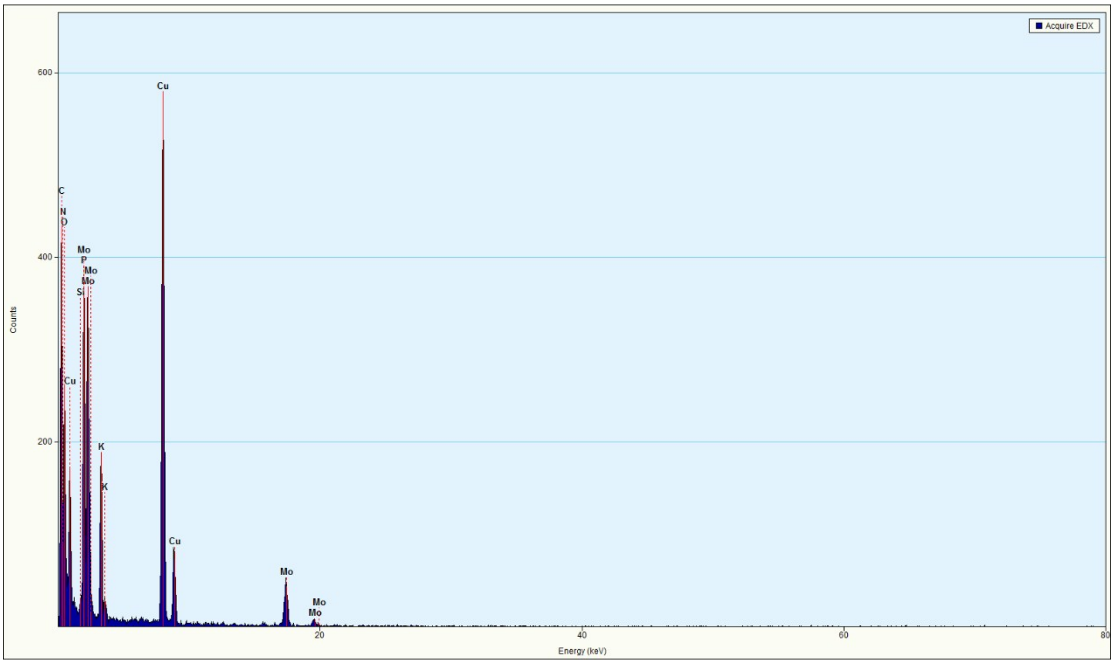

Figure S20. The EDS spectrum of MoP@NCF after long-term durability test in alkaline electrolyte.

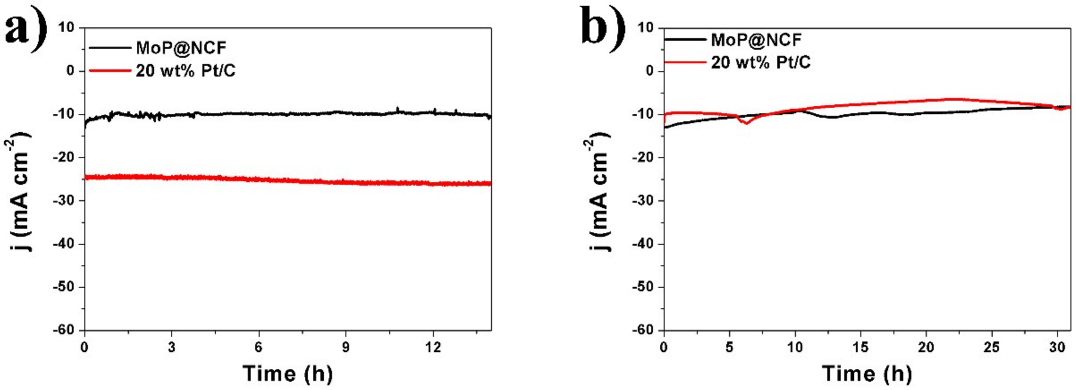

Figure S21. The durability comparison of MoP@NCF and the commercial 20 wt% Pt/C in both acid (a) and alkaline (b) electrolytes. The long-term durability of the commercial 20 wt% Pt/C was conducted at 50 mV vs. RHE in both acid and alkaline electrolytes.

Table S8. Comparison of the HER performance of some reported high performance MoP-based electrocatalysts in alkaline solution.

Electrocatalysts	**Electrolyte**	**Overpotential (mV) at 10 mV cm^{-2}**	**Tafel slope (mV dec^{-1})**	**Ref.**
MoP@NCF	1M KOH	129.5	72.4	This work
N-MoP	1M KOH	145	71.5	[3]
MoP@NPC-H	1M KOH	176	94	[4]
MoP/NPG	1M KOH	115	65	[5]
FLNPC@MoP-NC/MoP-C/CC	1M KOH	69	52	[6]
MoP@C	1M KOH	49	54	[7]
MoP NPs@NC	1M KOH	80	59	[8]
MoP/rGO	1M KOH	140	72	[9]

MoP/SN	1M KOH	94	59.7	10
MoP NA/CC	1M KOH	80	83	11
HF-MoSP	1M KOH	119	85	12
rGO-A-MoP	1M KOH	162	57	13
MoP-RGO nanoparticles	1M KOH	150	66	14

Table S9. Comparison of the HER performance of some reported high performance MoP-based electrocatalysts in acidic solution.

Electrocatalysts	**Electrolyte**	**Overpotential (mV) at 10 mV cm^{-2}**	**Tafel slope (mV dec^{-1})**	**Ref.**
MoP@NCF	0.5M H_2SO_4	121.8	74.5	This work
N-MoP	0.5M H_2SO_4	136	58.66	3
MoP@NPC-H	0.5M H_2SO_4	141	61	4
MoP/NPG	0.5M H_2SO_4	90	75	5
FLNPC@MoP-NC/MoP-C/CC	0.5M H_2SO_4	74	50	6
MoP@C	0.5M H_2SO_4	88	50.4	7
MoP NPs@NC	0.5M H_2SO_4	115	65	8
MoP/rGO	0.5M H_2SO_4	119	58	9

MoP/SN	0.5M H_2SO_4	104	45.49	10
MoP NA/CC	0.5M H_2SO_4	124	58	11
HF-MoSP	0.5M H_2SO_4	108	76	12
rGO-A-MoP	0.5M H_2SO_4	152	88	13
MoP-RGO nanoparticles	0.5M H_2SO_4	117	62	14
MoP/CNT	0.5M H_2SO_4	~114	51.6	15
MoP@HCC	0.5M H_2SO_4	129	48	16
MoP/NG	0.5M H_2SO_4	94	51	17
MoP|S	0.5M H_2SO_4	86	-	18
MoP-CA2	0.5M H_2SO_4	125	54	19
MoP@C@rGO	0.5M H_2SO_4	168.9	79	20
MoP@PC	0.5M H_2SO_4	258	59.3	21
MoP/CF	0.5M H_2SO_4	200	56.4	22
Bulk MoP	0.5M H_2SO_4	140	54	**23**

Reference

1. J. Li, J. Li, X. Wang, S. Zhang, J. Sha and G. Liu, *ACS Sustainable Chem. Eng.*, 2018, **6**, 10252-10259.
2. L. Xu, Q. Jiang, Z. Xiao, X. Li, J. Huo, S. Wang and L. Dai, *Angew. Chem. Int. Ed.*, 2016, **55**, 5277-5281.
3. L. Chai, W. Yuan, X. Cui, H. Jiang, J. Tang and X. Guo, *RSC Adv.*, 2018, **8**, 26871-26879.
4. J. Chi, W. Gao, L. Zhang, B. Dong, K. Yan, J. Lin, B. Liu, Y. Chai and C. Liu,

ACS Sustainable Chem. Eng., 2018, **6**, 7676-7686.

5. K. Lan, X. Wang, H. Yang, K. Iqbal, Y. Zhu, P. Jiang, Y. Tang, Y. Yang, W. Gao and R. Li, *ChemElectroChem*, 2018, **5**, 2256-2262.
6. B. Liu, H. Li, B. Cao, J. Jiang, R. Gao and J. Zhang, *Adv. Funct. Mater.*, 2018, **28**, 1801527.
7. G. Li, Y. Sun, J. Rao, J. Wu, A. Kumar, Q. Xu, C. Fu, E. Liu, G. R. Blake, P. Werner, B. Shao, K. Liu, S. Parkin, X. Liu, M. Fahlman, S. Liou, G. Auffermann, J. Zhang, C. Felser and X. Feng, *Adv. Energy Mater.*, 2018, **8**, 1801258.
8. Z. Pu, I. S. Amiinu, X. Liu, M. Wang and S. Mu, *Nanoscale*, 2016, **8**, 17256-17261.
9. H. Yan, Y. Jiao, A. Wu, C. Tian, X. Zhang, L. Wang, Z. Ren and H. Fu, *Chem. Commun.*, 2016, **52**, 9530-9533.
10. M. A. R. Anjum and J. S. Lee, *ACS Catal.*, 2017, **7**, 3030-3038.
11. Z. Pu, S. Wei, Z. Chen and S. Mu, *Appl. Catal. B*, 2016, **196**, 193-198.
12. A. Wu, C. Tian, H. Yan, Y. Jiao, Q. Yan, G. Yang and H. Fu, *Nanoscale*, 2016, **8**, 11052-11059.
13. K. Ojha, M. Sharma, H. Kolev and A. K. Ganguli, *Catal. Sci. Technol.*, 2017, **7**, 668-676.
14. Z. Wu, J. Wang, J. Zhu, J. Guo, W. Xiao, C. Xuan, W. Lei and D. Wang, *Electrochim. Acta*, 2017, **232**, 254-261.
15. A. Adam, M. H. Suliman, H. Dafalla, A. R. Al-Arfaj, M. N. Siddiqui and M. Qamar, *ACS Sustainable Chem. Eng.*, 2018, **6**, 11414-11423.
16. M. Hou, X. Teng, J. Wang, Y. Liu, L. Guo, L. Ji, C. Cheng and Z. Chen, *Nanoscale*, 2018, **10**, 14594-14599.
17. C. Huang, C. Pi, X. Zhang, K. Ding, P. Qin, J. Fu, X. Peng, B. Gao, P. K. Chu and K. Huo, *Small*, 2018, **14**, 1800667.
18. J. Kibsgaard and T. F. Jaramillo, *Angew. Chem. Int. Ed.*, 2014, **53**, 14433-14437.
19. Z. Xing, Q. Liu, A. M. Asiri and X. Sun, *Adv. Mater.*, 2014, **26**, 5702-5707.
20. Y. Zhang, J. Yang, Q. Dong, H. Geng, Y. Zheng, Y. Liu, W. Wang, C. Li and X. Dong, *ACS Appl. Mater. Interfaces*, 2018, **10**, 26258-26263.
21. J. Li, S. Zhang, J. Sha, H. Wang, M. Liu, L. Kong, and G. Liu, *ACS Appl. Mater. Interfaces*, 2018, **10**, 17140-17146.
22. W. Cui, Q. Liu, Z. Xing, A. M. Asiri , K. A. Alamry, and X. Sun, *Appl. Catal. B*, 2015, **164**, 144-150.
23. P. Xiao, M. A. Sk, L. Thia, X. Ge, R. J. Lim, J. Wang, K. H. Lim and X. Wang, *Energy Environ. Sci.*, 2014, **7**, 2624-2629.